

## **Supporting Information**

### **Distinguishing isobaric phosphated and sulfated carbohydrates by coupling of mass spectrometry with gas phase vibrational spectroscopy**

Baptiste Schindler, Janhavi Joshi, Abdul-Rahman Allouche, Daniel Simon, Stéphane Chambert, Vincent Brites, Marie-Pierre Gageot, and Isabelle Compagnon

## **A) Experimental methods**

**Samples:** Solid samples of D-Glucosamine 6-Phosphate and D-Glucosamine 6-Sulfate (>98%) were obtained from Sigma-Aldrich and used without further purification. 250  $\mu$ M solution were prepared in a mixture of H<sub>2</sub>O/Methanol (50:50).

**Mass spectrometry:** A ThermoFinnigan LCQ instrument (3-D ion trap) coupled with an electrospray ion source (ESI) is used for mass spectrometry. The liquid sample are directly infused to obtain the full mass spectrum of the protonated ions. The ions of interest are further isolated (MS<sub>2</sub>) and undergo dissociation under soft collision conditions in the Helium buffer of the 3D-ion trap (CID).

**IR spectroscopy:** The commercial mass spectrometer is modified to allow laser spectroscopy of the isolated ions. A sapphire window is placed on top of the ring electrode of the ion trap to allow laser irradiation of the ion cloud. The laser is synchronized with the second phase of the MS<sub>2</sub> sequence, in order to ensure that only the ions of interest are irradiated. The vibrational spectra of the individual mass-selected ions are recorded by monitoring the laser induced Infrared Multiple Photon Dissociation (IRMPD) as a function of the excitation wavelength in the 2850-3700  $\text{cm}^{-1}$  spectral range, using a yag-pump tunable IR OPO/OPA laser (laser Vision).

**IR spectroscopy using FEL:** the same principle is used to record vibrational spectra in the mid-IR range (1000-2000  $\text{cm}^{-1}$ ). The setup, consisting of a FT-ICR high resolution mass spectrometer modified to allow injection of a free electron laser beam on the ion cloud, is available as part of the laser facility CLIO (University Paris Sud-Orsay).

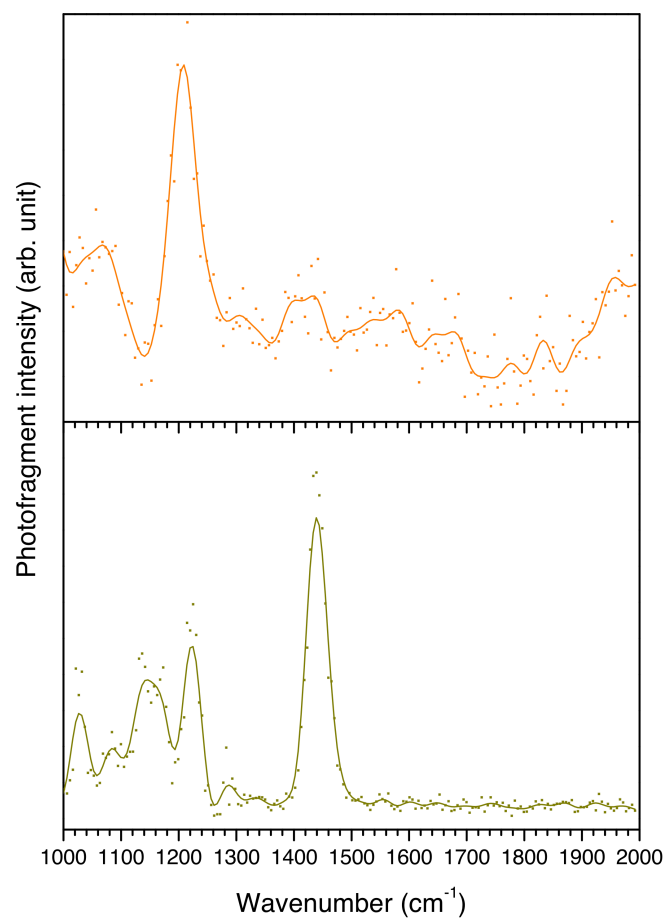


**Figure S1:** the mid-IR spectra of protonated D-Glucosamine 6-Phosphate (orange) and D-Glucosamine 6-Sulfate (dark yellow) display no feature at the expected position of C=O stretching, which is a strong indication of the presence of a cyclic form.

## **B) Ab initio calculations**

**Conformational search:** The conformational search was done by molecular dynamics calculations using the PM7 [PM7] semi-empirical potential, followed by a geometry optimization using the same semi-empirical method. Finally, a Density Functional Theory (DFT) geometry optimization was done. The semi-empirical PM7 potential was chosen for its good chemical accuracy especially for hydrogen-bonding interactions. Indeed, the monosaccharides are very rich in OH groups and, at low temperature, hydrogen bonds can be formed to give rise to stabilization of the structure. For each molecule, an initial geometry was first optimized using the PM7 method. The molecular dynamics simulations were performed using the Velocity Verlet algorithm [Verlet] with a time step of 0.5 fs and a simulation time of 10 ps and a temperature of 3000 K. The high temperature was chosen to provide an exhaustive exploration of the potential energy surface. We selected 1000 geometries at regular time intervals during the production steps of the simulation. At the end of the molecular dynamic simulation, the selected geometries were optimized using the PM7 semi-empirical method. Similar geometries were removed (two geometries are considered similar if the difference between their energies is less than 0.1 kcal/mol and the difference between their distances less than 0.1 angstrom including non-bonded atoms). After which, the optimized geometries were reoptimized using the B3LYP/6-31+G\*. Finally all these geometries were optimized at the B3LYP/6-311+G\* level of theory.

**Conformational analysis.** Semi empirical conformational search with PM7 method followed by DFT geometry optimization at the B3LYP/6-311+G\* level yielded circa 200 structures for each of the four pyranose forms of interest with a fixed protonation site on the amide function, namely  $\alpha$ -D-Glucosamine 6-Phosphate,  $\beta$ -D-Glucosamine 6-Phosphate,  $\alpha$ -D-Glucosamine 6-Sulfate,  $\beta$ -D-Glucosamine 6-Sulfate. Both alpha and beta anomeric forms were addressed since they co-exist in solution.

### **Simulation of Infrared spectra**

Harmonic simulations of the infrared spectra were calculated at B3LYP/6-311+G\* level. For the most stable geometry, VPT2 [VPT2] was used to compute the anharmonicity effect.

## Additional, high energy conformers

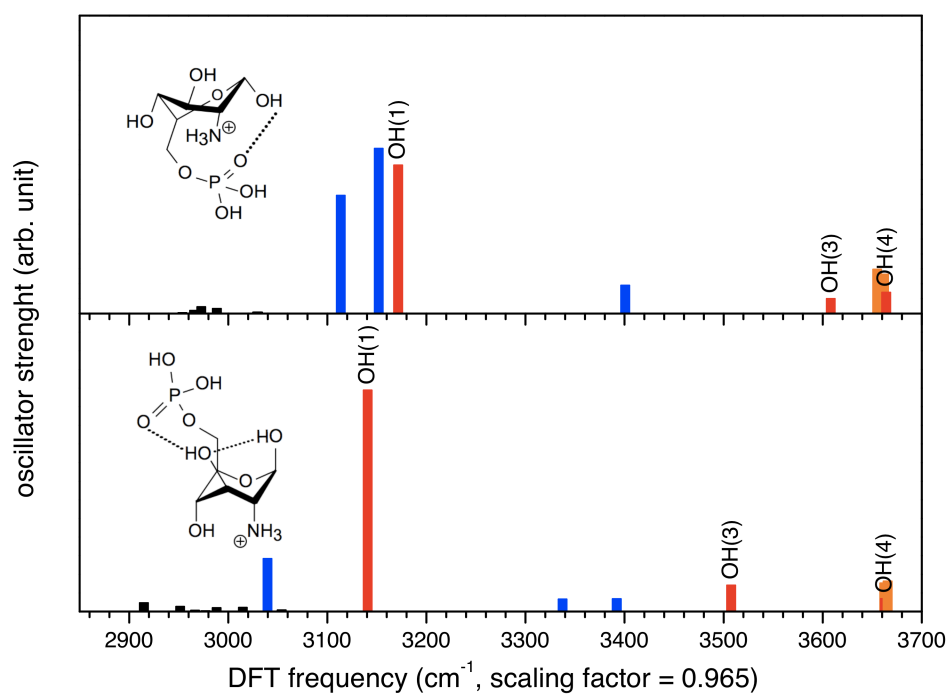


**Figure S2:**  $\beta$ -Glucosamine 6-Phosphate adopts an additional 1C4 conformation stabilized by two H-bonds between P=O, OH(1) and OH(3). A skew 1S5 form was marginally observed for  $\alpha$ -Glucosamine 6-Phosphate.

### C) DFT-MD simulations

The calculations of the IR spectra of phosphate and sulfate glucosamine were done through DFT-based molecular dynamics simulations performed with the CP2K package [CP2K]. We used the BLYP functional [B,LYP] including Grimme D3 correction for dispersion [D3] combined with Goedecker-Tetter-Hutter (GTH) pseudopotentials [PP1,PP2], the TZV2P-GTH Gaussian basis set for all atoms, a plane-wave density cut-off of 450 Ry, and a cubic cell with a length of 20 Å in each direction. The dynamics were performed in the NVE ensemble with a time-step of 0.4 fs, and were divided into an equilibration period of 3 ps in which the atomic velocities can be rescaled (with a targeted temperature of 300 K  $\pm$  40 K), and a production period of 8 ps where the individual infrared spectra are accumulated. The dynamical infrared spectra are then calculated through the Fourier transform of the dipole-dipole correlation function [MPG] and assigned in terms of atomic displacements through VDOS (Velocity Density of States) analysis calculated as the Fourier transform of velocity correlation functions [MPG]. Both  $\alpha$ - and  $\beta$ -anomers are investigated separately (separate trajectories) and the final IR spectra resulted from the addition of the individual spectra. Figures S3 and S4 respectively present the individual and combined spectra of the phosphated and sulfated species. Comparison with experiment is reported on Figure S5.

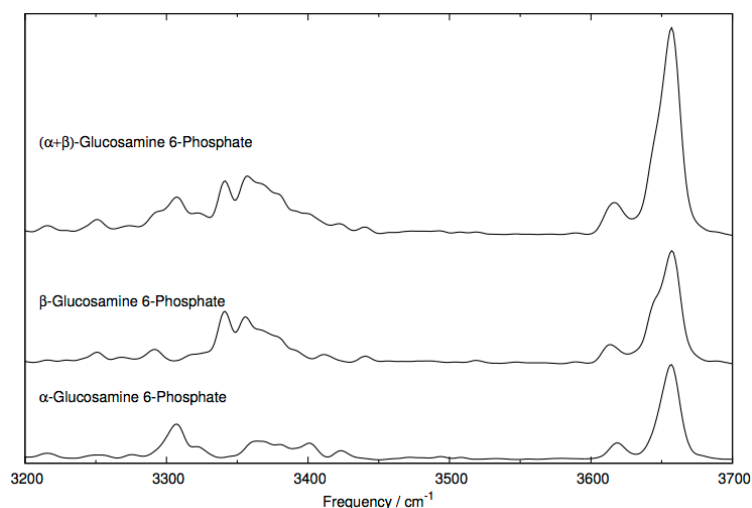


**Figure S3.** Dynamical IR spectra of Glucosamine 6-Phosphate calculated at 300 K: alpha- and beta-anomers spectra presented separately, and their sum (as in the paper).

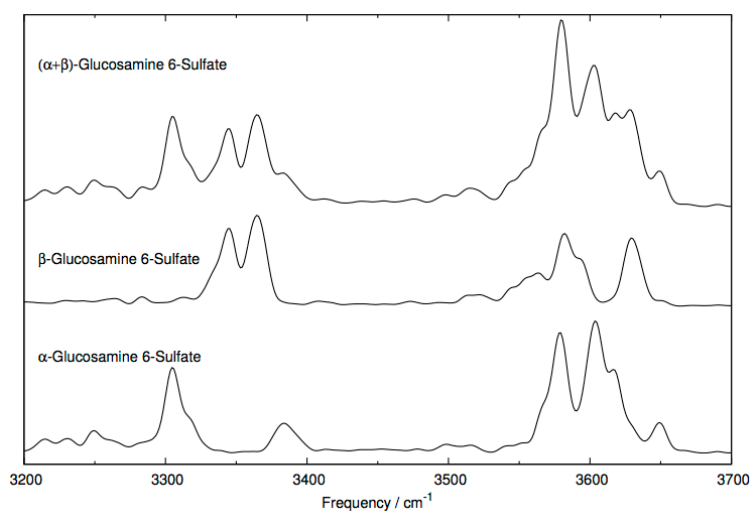


**Figure S4.** Dynamical IR spectra of Glucosamine 6-Sulfate calculated at 300 K: alpha- and beta-anomers spectra presented separately, and their sum (as in the paper).

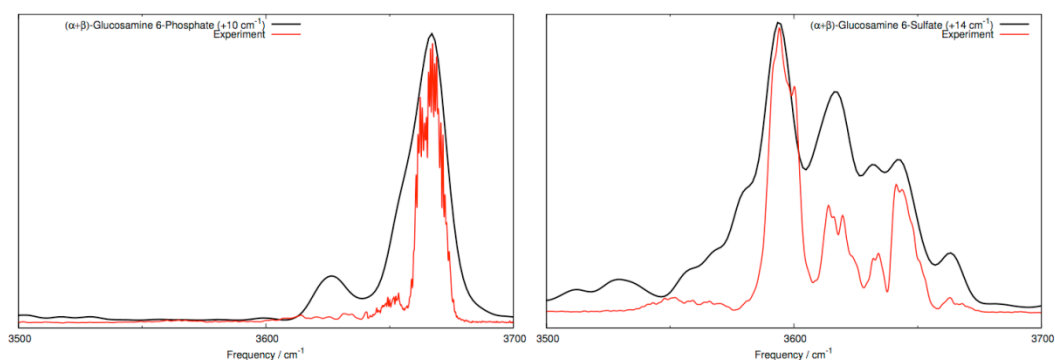


**Figure S5.** Comparison between the combined ( $\alpha + \beta$ ) dynamical IR spectra computed at 300 K and the IR-MPD experiment. For Glucosamine 6-Phosphate (left), the calculated spectrum is shifted by  $+10 \text{ cm}^{-1}$ . For of Glucosamine 6-Sulfate (right), the calculated spectrum is shifted by  $+14 \text{ cm}^{-1}$ .

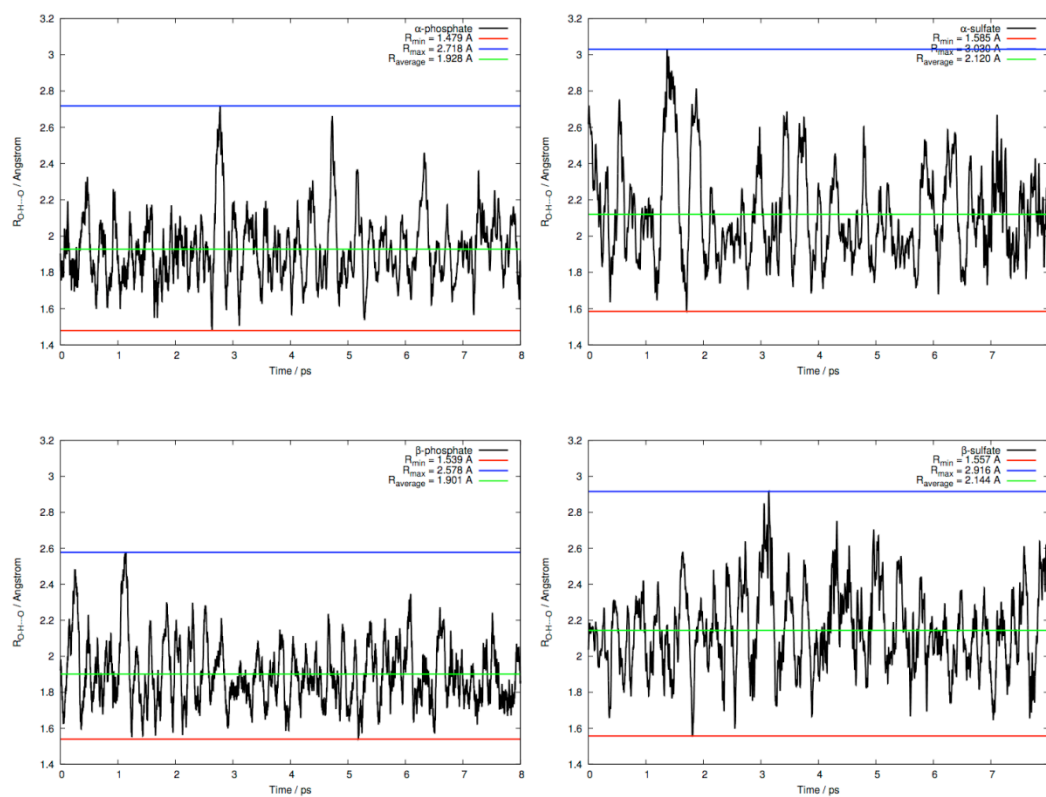


**Figure S6.** Evolution with time of the hydrogen bond distance between the oxygen of the function and the OH(4) of the ring during the 8 ps of dynamics. The minimum, average, and maximum values are reported by a red, green, and blue line, respectively. These plots support the main text of the paper for the discussion on “strong” and “weaker” H-bonds formed between the function and the OH(4) on average.



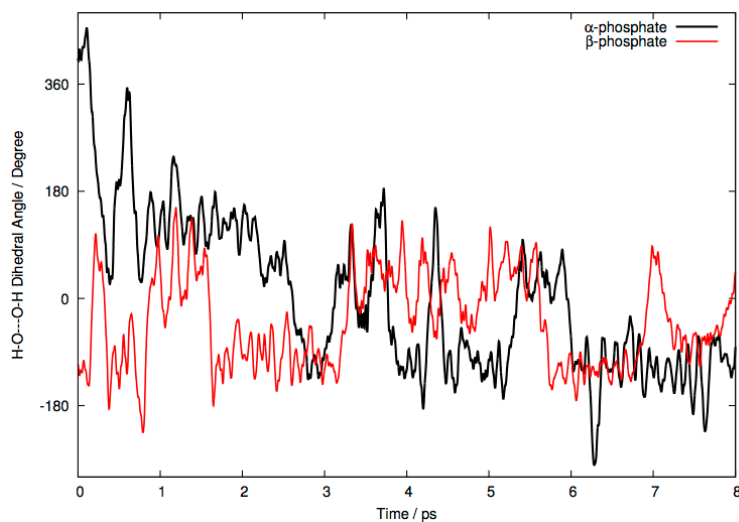


**Figure S7.** Evolution with time of the dihedral H-O...O-H angle between the two OH groups of the function for the phosphated species during the 8 ps of dynamics. Values around  $0^\circ$  and  $360^\circ$  correspond to a “cis” orientation of these two groups, whereas  $180^\circ$  and  $-180^\circ$  correspond to a “trans” orientation of these two groups.

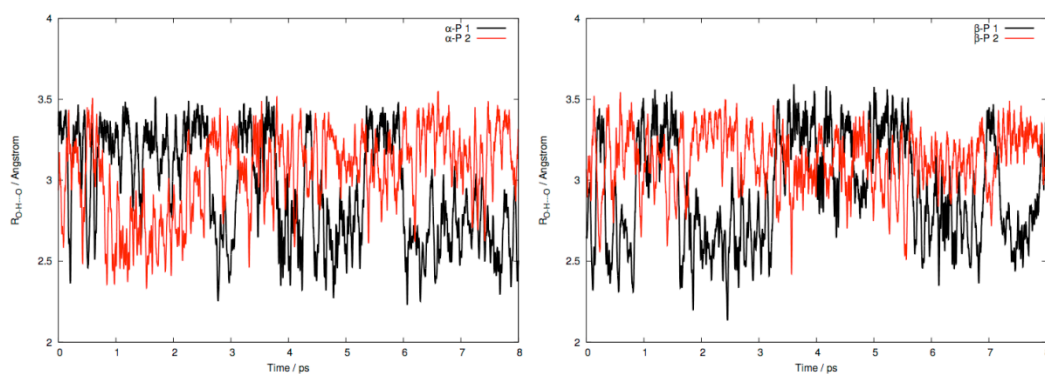


**Figure S8.** Evolution with time of the O-H...O distances angle between the two OH groups of the function for the phosphated species during the 8 ps of dynamics.

Figures S7 and S8 are related to the two OH groups of the phosphate function in the alpha- and beta-anomers of the phosphated saccharide. Figure S7 shows that at room temperature, the structure is not frozen at a given structure, but instead the two OH groups have a continuous rotational motion. As a consequence, one cannot think of Glucosamine 6-Phosphate saccharide as a rigid molecule from the point of view of the two OH groups carried by the phosphate function, but instead one has to think of the molecule as a dynamical one, especially from the point of view of these functional OH groups. This has already been observed for a similar phosphate group in a different environment [CIMAS]. If this rotational motion is not taken into account for the spectra calculations, as it is the case in the harmonic calculations or in the VPT2 anharmonic calculations, then the final spectral signatures of these OH groups are not correct. This is the strength of the dynamical spectra calculated here, as they take this finite temperature rotational motion into account in the final spectral signatures, providing an excellent agreement with the experiment.

Figure S8 shows the evolution with time of the O-H...O-H distance between the two OH groups of the phosphate function. It illustrates that there are no H-bonds formed between these two groups along the time, the continuous rotational motion observed above prevents any such hydrogen bonding.

## References

- [PM7] Journal of Molecular Modeling January 2013, Volume 19, Issue 1, pp 1-32.
- [Verlet] W.C. Swope, H.C. Andersen, P.H. Berens, and K.R. Wilson, *J. Chem. Phys.* **76**, 637 (1982).
- [VPT2] V. Barone, "Anharmonic vibrational properties by a fully automated second-order perturbative approach," *J. Chem. Phys.*, **122** (2005) 014108: 1-10.
- [CP2K] CP2K version 2.4.0, the CP2K developers group (2013). CP2K is freely available from <http://www.cp2k.org/>.
- [MPG] Gageot, M.-P.; Theoretical spectroscopy of floppy peptides at room temperature. A DFTMD perspective: gas and aqueous phase, *Phys. Chem. Chem. Phys.* **2010**, *12*, 3336.
- [B] Becke, A.D.; Density-functional exchange-energy approximation with correct asymptotic behavior, *Phys. Rev. A* **1988**, *38*, 3098.
- [LYP] Lee, C.; Yang, W.; Parr, R.G.; Development of the Colle-Salvetti correlation-energy formula into a functional of the electron density, *Phys. Rev. B* **1988**, *37*, 785.
- [D3] Grimme, S.; Antony, J.; Ehrlich, S.; Krieg, H.; A consistent and accurate ab initio parametrization of density functional dispersion correction (DFT-D) for the 94 elements H-Pu, *J. Chem. Phys.* **2010**, *132*, 154104.
- [PP1] Goedecker, S.; Teter, M.; Hutter, J.; Separable dual-space Gaussian pseudopotentials, *Phys. Rev. B* **1996**, *54*, 1703.
- [PP2] Krack, M.; Pseudopotentials for H to Kr optimized for gradient-corrected exchange-correlation functionals, *Theor. Chem. Acc.* **2005**, *114*, 115.
- [CIMAS] Cimas, A.; Maitre, P.; Ohanessian, G.; Gageot, M.-P.; Molecular Dynamics and Room Temperature Vibrational Properties of Deprotonated Phosphorylated Serine, *J. Chem. Theory. Comput.* **2009**, *5*, 2388.